Journal of Statistics: Advances in Theory and Applications
Volume 2, Number 1, 2009, Pages 93-111

A SIMULATION STUDY OF THE COVARIANCE AND CORRELATION PROPERTIES OF THE FRACTIONALLY INTEGRATED SEPARABLE SPATIAL AUTOREGRESSIVE (FISSAR) MODEL

MAHENDRAN SHITAN and TENG MEI TUAN

Department of Mathematics
Faculty of Science
Universiti Putra Malaysia
Malaysia
e-mail: mahen698@gmail.com

Applied & Computational Statistics Laboratory
Institute for Mathematical Research
Universiti Putra Malaysia
Malaysia

Abstract

Spatial modelling has its applications in many fields. In time series, there exists a class of models known as long memory models, where the autocorrelation function decays rather slowly. These types of time series data are modelled as fractionally integrated ARMA processes. Spatial data may also exhibit a long memory structure and in order to model such structure, a class of models called as the *Fractionally Integrated Separable Spatial Autoregressive* (FISSAR) Model has been introduced. The objectives of this research are to demonstrate on how to

2000 Mathematics Subject Classification: 62M30.

Keywords and phrases: fractionally integrated process, autoregressive process, separable models, spatial model, variance, covariance, correlation.

Received September 14, 2009

simulate a FISSAR (1, 1) process, to examine the properties of the variance estimator and to illustrate the correlation properties.

1. Introduction

Spatial modelling has its applications in many fields like geology, geography, agriculture, meteorology, etc. Spatial data can be classified as geostatistical data, lattice data, or point patterns. These differences are due to whether the spatial data has been observed on a continuous domain or at discrete locations. In point pattern analysis, the domain is random and interest focusses on the location of events.

In this paper, we concentrate on lattice data observed on a regular grid. Many models have been suggested in modelling spatial dependence like the Simultaneous Autoregression (SAR) (Whittle [16]), Conditional Autoregression (CAR) (Bartlett [1], and Besag [4]), Moving Average (MA) (Haining [9]), and Unilateral models (Basu and Reinsel [3]).

There exists another class of models that are known as *separable* models, which has the property of a reflection symmetric correlation structure, (i.e., $\rho_{h,k} = \rho_{-h,-k} = \rho_{h,-k} = \rho_{-h,k}$). This type of model is also known as linear by linear process (Martin [11]) and its correlation structure can be expressed as a product of correlations, (i.e., $\rho_{x,h,k} = \rho_{y,h}\rho_{z,k}$). Basawa et al. [2] have considered separable models on k-dimensional lattice and have shown that the correlation structure is $\rho(\mathbf{h}) = \prod \rho_i(h_i)$.

In area of time series, there exists a class of models known as long memory models, where the autocorrelation function decays rather slowly. These types of time series data are modelled as fractionally integrated ARMA processes (see Brockwell and Davis [6] & [7]). The usefulness of time series long memory models have been applied in various diverse fields (Hurst [10]), Granger [8], Shitan and Wee [12], Shitan et al. [13]).

It is conceivable that in some cases spatial data may also exhibit a long memory structure. Boissy et al. [5] had extended the long memory concept from time series to the spatial context and introduced the fractional autoregressive model given as,

$$\phi(B_1, B_2, \alpha, \beta)\nabla^d X_{st} = \varepsilon_{st},$$

where $\nabla^d = (1 - B_1)^{d_1}(1 - B_2)^{d_2}$. Independently, Shitan [14, 15] worked on a similar model and termed it the Fractionally Integrated Separable Spatial Autoregressive (FISSAR) model as it is possible to construct a *non-separable* counterpart.

Hence, in this paper, we discuss on (i) how to simulate the FISSAR (1, 1) process, (ii) the variance estimator through a simulation study, and (iii) the decaying nature of the correlation function which is illustrated graphically.

In Section 2 of this paper, the simulation of FISSAR (1, 1) process is discussed in detail, while in Section 3, we deal with the variance of the FISSAR (1, 1) process. In Section 4, we compute the correlation function and illustrate graphically its decaying nature. Finally, the conclusions are drawn in Section 5.

2. Simulation of the FISSAR (1, 1) Process

In this section, we provide and discuss two methods of simulating the FISSAR (1, 1) process.

The FISSAR model is defined as follows (See Shitan [14]). Let $\{Y_{ij}\}$ be a sequence of spatial observations on a two dimensional *regular* lattice that satisfies the following equation.

$$(1 - \phi_{10}B_1 - \phi_{01}B_2 + \phi_{10}\phi_{01}B_1B_2)(1 - B_1)^{d_1}(1 - B_2)^{d_2} Y_{ij} = Z_{ij}, \qquad (1)$$

where B_1 is the usual backward shift operator acting in the i-th direction, B_2 is the backward shift operator acting in the j-th direction, $\{Z_{i,j}\}$ is a two dimensional white noise process with mean zero and variance σ^2 and $-0.5 < d_1, d_2 < 0.5$.

Method 1

In order to show how to simulate a FISSAR (1, 1) process, we begin with the defining equation of FISSAR (1, 1) model (Equation (1)).

Using binomial expansions, we can rewrite the Equation (1) as,

$$(1 - \phi_{10}B_1 - \phi_{01}B_2 + \phi_{10}\phi_{01}B_1B_2)\left(\sum_{k=0}^{\infty}\pi_k B_1^k\right)\left(\sum_{l=0}^{\infty}\psi_l B_2^l\right)Y_{ij} = Z_{ij},$$

where π_k and ψ_l are given as,

$$\pi_k = \frac{\Gamma(k - d_1)}{\Gamma(k+1)\Gamma(-d_1)}, \quad \psi_l = \frac{\Gamma(l - d_2)}{\Gamma(l+1)\Gamma(-d_2)}.$$

After some algebraic manipulation, it can be shown that,

$$\begin{aligned} Y_{ij} = Z_{ij} &- \sum_{k=1}^{\infty}\pi_k Y_{i-k,j} - \sum_{l=1}^{\infty}\psi_l Y_{i,j-l} - \sum_{k=1}^{\infty}\sum_{l=1}^{\infty}\pi_k\psi_l Y_{i-k,j-l} \\ &+ \phi_{10}\sum_{k=0}^{\infty}\sum_{l=0}^{\infty}\pi_k\psi_l Y_{i-k-1,j-l} + \phi_{01}\sum_{k=0}^{\infty}\sum_{l=0}^{\infty}\pi_k\psi_l Y_{i-k,j-l-1} \\ &- \phi_{10}\phi_{01}\sum_{k=0}^{\infty}\sum_{l=0}^{\infty}\pi_k\psi_l Y_{i-k-1,j-l-1}. \end{aligned} \tag{2}$$

Now, we can simulate a FISSAR (1, 1) process by first generating a sequence of $\{Z_{ij}\}$ followed by $\{Y_{ij}\}$ according to Equation (2) by truncating at some point. The truncation points for the infinite sums used in this study is fifty (50). In order to reduce the effects of the initial value and border effects, we need to generate a sufficiently large data set and use only the interior values of the spatial grids.

Method 2

Equation (1) can equivalently be represented by the following two equations.

$$(1 - \phi_{10}B_1 - \phi_{01}B_2 + \phi_{10}\phi_{01}B_1B_2)Y_{ij} = W_{ij}, \tag{3}$$

and

$$(1 - B_1)^{d_1}(1 - B_2)^{d_2}W_{ij} = Z_{ij}. \tag{4}$$

We shall call the process $\{W_{ij}\}$ as two dimensional fractionally integrated white noise. Notice that $(1 - \phi_{10}B_1 - \phi_{01}B_2 + \phi_{10}\phi_{01}B_1B_2)$ can be factored out as $(1 - \phi_{10}B_1)(1 - \phi_{01}B_2)$ and this is known as a *separable* process.

Now, we can simulate a FISSAR (1, 1) process in two stages. Firstly, we generate a sequence of $\{Z_{ij}\}$, and then by using Equation (4), we generate the sequence $\{W_{ij}\}$. Finally, using Equation (3), we obtain the sequence $\{Y_{ij}\}$. Since, the expansions involve infinite sums a truncation at some point is required. The truncation points for the infinite sums used in this study are fifty (50). In this study for both simulation methods, we generated grid size 50×50, but used only the interior values of grid size 30×30 (south east corner).

A typical sample realisation of the FISSAR (1, 1) model with $\phi_{10} = 0.1$, $\phi_{01} = 0.1$, $d_1 = 0.1$, and $d_2 = 0.1$ is shown in Figure 1. Further, examples of simulation with differing parameter values are discussed in the results section (Section 4).

The two simulation methods are equivalent in the sense that they would produce exactly the same data values for a given set of parameter values. However, the second method of simulation would be computationally faster and hence the second method would be preferred.

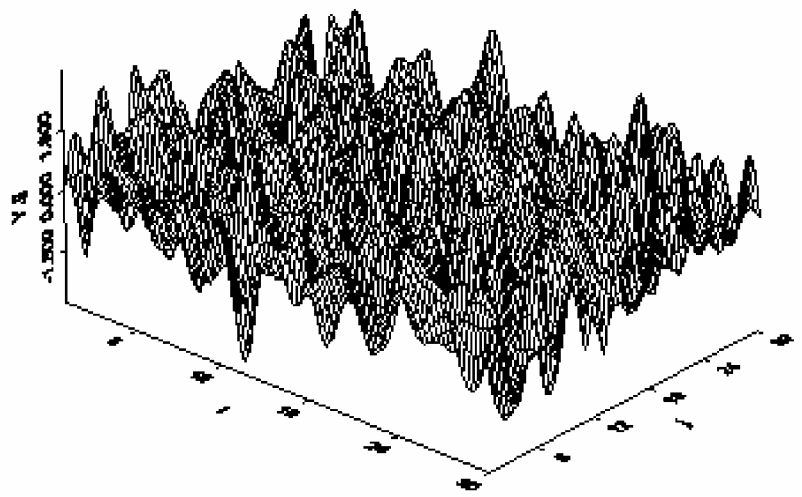

Figure 1. FISSAR sample realisation: $\phi_{10} = 0.1$, $\phi_{01} = 0.1$, $d_1 = 0.1$, and $d_2 = 0.1$.

3. Variance of the FISSAR (1, 1) Process

In Subsection 3.1, the theoretical variance of the FISSAR (1, 1) process is discussed, and in Subsection 3.2, an estimator of the variance is provided.

3.1. Theoretical variance

The theoretical variance of the FISSAR (1, 1) process is given as,

$$\gamma_Y(0, 0) = \sum_{k=0}^{\infty}\sum_{l=0}^{\infty}\sum_{m=0}^{\infty}\sum_{n=0}^{\infty}\phi_{10}^{k+m}\phi_{01}^{l+n}\gamma_W(k-m, l-n), \tag{5}$$

where $\gamma_W(k-m, l-n)$ is given as,

$$\sigma^2 \frac{(-1)^{k-m+l-n}\Gamma(1-2d_1)\Gamma(1-2d_2)}{\Gamma(k-m-d_1+1)\Gamma(1-k+m-d_1)\Gamma(l-n-d_2+1)\Gamma(1-l+n-d_2)},$$

(see Shitan [14]).

Since, the theoretical variance involves computation of infinite sums, we have therefore, computed the *approximate* theoretical variance for some selected values of the parameters of the FISSAR (1, 1) model using Equation (5). The cut off points in the computation of Equation (5) is 100 for each of the summations, while the selected parameter values are $\phi_{10} = 0.1$, $\phi_{01} = 0.1$, $\sigma^2 = 1.0$, while d_1 and d_2 are allowed to vary from -0.4 to 0.4. These approximate theoretical variances are listed out in Table 1.

Table 1. Theoretical variance for some selected values of the FISSAR (1, 1) model $(\phi_{10} = 0.1, \phi_{01} = 0.1, \sigma^2 = 1.0)$

$d_1 : d_2$	−0.4	−0.3	−0.2	−0.1	0	0.1	0.2	0.3	0.4
−0.4	1.2656	1.2005	1.1546	1.1309	1.1363	1.1858	1.3154	1.6349	2.6962
−0.3	1.2005	1.1388	1.0952	1.0728	1.0779	1.1249	1.2478	1.5509	2.5577
−0.2	1.1546	1.0952	1.0533	1.0317	1.0367	1.0818	1.2000	1.4915	2.4597
−0.1	1.1309	1.0728	1.0317	1.0105	1.0154	1.0596	1.1754	1.4609	2.4092
0	1.1363	1.0779	1.0367	1.0154	1.0203	1.0648	1.1811	1.4679	2.4209
0.1	1.1858	1.1249	1.0181	1.0596	1.0648	1.1111	1.2326	1.5319	2.5264
0.2	1.3154	1.2478	1.2000	1.1754	1.1811	1.2326	1.3672	1.6993	2.8024
0.3	1.6349	1.5509	1.4915	1.4609	1.4679	1.5319	1.6993	2.1120	3.4830
0.4	2.6962	2.5577	2.4597	2.4092	2.4209	2.5264	2.8024	3.4830	5.7441

It can be seen that Table 1 is a symmetric matrix. Now for a fixed row, the values initially decrease as we proceed from left to right, attains a minimum, and then the values increase. In short, it has a quadratic shaped curve. Similarly, for a fixed column, as we proceed from top to bottom, we observe that the variance decreases, attains a minimum, and then increases again. Hence, along the column, the variance also has a quadratic shaped curve.

Table 2 shows the theoretical variance for some selected values of the parameters of the FISSAR (1, 1) model computed by using Equation (5), where we have fixed $\phi_{10} = 0.3$, $\phi_{01} = 0.3$, and $\sigma^2 = 1.0$. The parameters d_1 and d_2 are allowed to vary from -0.4 to 0.4.

Table 2. Theoretical variance for some selected values of the FISSAR (1, 1) model $(\phi_{10} = 0.3, \phi_{01} = 0.3, \sigma^2 = 1.0)$

$d_1 : d_2$	−0.4	−0.3	−0.2	−0.1	0	0.1	0.2	0.3	0.4
−0.4	1.1186	1.0914	1.0847	1.1045	1.1622	1.2815	1.5189	2.0453	3.7187
−0.3	1.0914	1.0648	1.0583	1.0777	1.1339	1.2503	1.4819	1.9955	3.6282
−0.2	1.0847	1.0583	1.0519	1.0711	1.1270	1.2427	1.4729	1.9834	3.6061
−0.1	1.1045	1.0777	1.0711	1.0907	1.1476	1.2654	1.4998	2.0196	3.6720
0	1.1622	1.1339	1.1270	1.1476	1.2076	1.3315	1.5782	2.1251	3.8638
0.1	1.2815	1.2503	1.2427	1.2654	1.3315	1.4682	1.7402	2.3433	4.2604
0.2	1.5189	1.4819	1.4729	1.4998	1.5782	1.7402	2.0625	2.7773	5.0496
0.3	2.0453	1.9955	1.9834	2.0196	2.1251	2.3433	2.7773	3.7398	6.7996
0.4	3.7187	3.6282	3.6061	3.6720	3.8638	4.2604	5.0496	6.7996	12.3628

Again, we notice that Table 2 is a symmetric matrix and for a fixed row, the variance initially decreases as we proceed from left to right. It attains a minimum, and then the values increases. For a fixed column, as we proceed from top to bottom, we observe a similar pattern, where the variance decreases attaining a minimum, and then increases again.

3.2. Estimation of the variance

Given a spatial data set $\{y_{ij}\}$ on an m by n regular grid, an estimate of $\gamma_Y(0, 0)$ is given as,

$$\hat{\gamma}_Y(0, 0) = \frac{1}{mn} \sum_{i=1}^{m} \sum_{j=1}^{n} (y_{ij} - \bar{y}..)^2, \tag{6}$$

where $\bar{y}.. = \frac{1}{mn} \sum_{i=1}^{m} \sum_{j=1}^{n} y_{ij}$. In Subsection 3.3, we discuss the simulation results of the estimator provided by Equation (6).

3.3. Simulation results for the variance estimator

We simulated several sets of 50×50 spatial grid of the FISSAR (1, 1) model with the following parameter values.

(i) $\phi_{10} = 0.1, \phi_{01} = 0.1, d_1 = -0.4, d_2 = -0.4, \sigma^2 = 1.0,$

(ii) $\phi_{10} = 0.1,\ \phi_{01} = 0.1,\ d_1 = -0.4,\ d_2 = -0.3,\ \sigma^2 = 1.0,$

(iii) $\phi_{10} = 0.1,\ \phi_{01} = 0.1,\ d_1 = -0.4,\ d_2 = 0.4,\ \sigma^2 = 1.0,$

(iv) $\phi_{10} = 0.1,\ \phi_{01} = 0.1,\ d_1 = 0.1,\ d_2 = 0.1,\ \sigma^2 = 1.0,$

(v) $\phi_{10} = 0.1,\ \phi_{01} = 0.1,\ d_1 = 0.3,\ d_2 = 0.4,\ \sigma^2 = 1.0,$

(vi) $\phi_{10} = 0.1,\ \phi_{01} = 0.1,\ d_1 = 0.4,\ d_2 = 0.4,\ \sigma^2 = 1.0.$

We then took the 30×30 interior values (south east corner) of the spatial grid for studying the properties of the FISSAR (1, 1) model. We computed the sample variance using Equation (6) and carried out the following computations in our simulation study, where we let s be the number of simulations.

(i) Mean, $\bar{\hat{\gamma}}_Y(0, 0) = \frac{1}{s}\sum_{i=1}^{s}\hat{\gamma}_{Y,i}(0, 0),$

(ii) Estimated Bias $= \bar{\hat{\gamma}}_Y(0, 0) - \gamma_Y(0, 0),$

(iii) Estimated Standard Errors $= \sqrt{\frac{1}{s-1}\sum_{i=1}^{s}(\hat{\gamma}_{Y,i}(0, 0) - \bar{\hat{\gamma}}_Y(0, 0))^2},$

(iv) Estimated Root Mean Square Errors (RMSE)

$$= \sqrt{\frac{1}{s}\sum_{i=1}^{s}(\hat{\gamma}_{Y,i}(0, 0) - \gamma_Y(0, 0))^2}.$$

In this study, s was fixed at 100 and the results of the above computations are contained in Table 3.

The smallest absolute estimated bias occurred at $d_1 = -0.4,$ and $d_2 = -0.3.$ For other values of d_1 and $d_2,$ the bias was negative. We observed that the absolute estimated bias appears to be smaller for negative values of d_1 and d_2 than for the corresponding positive values of d_1 and $d_2.$ For instance, the absolute estimated bias is 0.0051 for $d_1 = -0.4,$ and $d_2 = -0.4,$ but the absolute estimated bias is 2.9488 for $d_1 = 0.4,$ and $d_2 = 0.4.$

The smallest estimated standard error was observed for $d_1 = 0.1$, and $d_2 = 0.1$. The smallest RMSE value also occurred for $d_1 = 0.1$, and $d_2 = 0.1$. Once again, the estimated RMSE values appears to be larger for positive values of d_1 and d_2 compared with the corresponding negative values of d_1 and d_2.

We also simulated several sets of 50×50 spatial grid of the FISSAR (1, 1) model with the following parameter values.

Table 3. Simulation results for $\hat{\gamma}_Y(0, 0)$

$(\phi_{10} = 0.1, \phi_{01} = 0.1, \sigma^2 = 1.0)$

	$d_1 = -0.4$ $d_2 = -0.4$	$d_1 = -0.4$ $d_2 = -0.3$	$d_1 = -0.4$ $d_2 = 0.4$	$d_1 = 0.1$ $d_2 = 0.1$	$d_1 = 0.3$ $d_2 = 0.4$	$d_1 = 0.4$ $d_2 = 0.4$
Theoretical Variance $\gamma_Y(0, 0)$	1.2656	1.2005	2.6962	1.1111	3.4830	5.7441
Mean $\bar{\hat{\gamma}}_Y(0, 0)$	1.2605	1.2023	1.9891	1.0968	2.2556	2.7953
Estimated Bias	−0.0051	0.0018	−0.7071	−0.0143	−1.2274	−2.9488
Absolute Estimated Bias	0.0051	0.0018	0.7071	0.0143	1.2274	2.9488
Estimated Standard Errors	0.0745	0.1112	0.2101	0.0602	0.2581	0.3774
Estimated RMSE	0.0743	0.1107	0.7374	0.0616	1.2540	2.9726

(i) $\phi_{10} = 0.3$, $\phi_{01} = 0.3$, $d_1 = -0.4$, $d_2 = -0.4$, $\sigma^2 = 1.0$,

(ii) $\phi_{10} = 0.3$, $\phi_{01} = 0.3$, $d_1 = -0.4$, $d_2 = -0.3$, $\sigma^2 = 1.0$,

(iii) $\phi_{10} = 0.3$, $\phi_{01} = 0.3$, $d_1 = -0.4$, $d_2 = 0.4$, $\sigma^2 = 1.0$,

(iv) $\phi_{10} = 0.3$, $\phi_{01} = 0.3$, $d_1 = 0.1$, $d_2 = 0.1$, $\sigma^2 = 1.0$,

(v) $\phi_{10} = 0.3$, $\phi_{01} = 0.3$, $d_1 = 0.3$, $d_2 = 0.4$, $\sigma^2 = 1.0$,

(vi) $\phi_{10} = 0.3$, $\phi_{01} = 0.3$, $d_1 = 0.4$, $d_2 = 0.4$, $\sigma^2 = 1.0$.

Similar computations using (i) to (iv) were carried out and the results are presented in Table 4.

From Table 4, we observed that the smallest absolute estimated bias occurred at $d_1 = -0.4$, and $d_2 = -0.4$. However, for the estimated standard error, the smallest value occurred at $d_1 = -0.4$, and $d_2 = -0.3$. The estimated RMSE was smallest for $d_1 = -0.4$, and $d_2 = -0.3$.

Table 4. Simulation results for $\hat{\gamma}_Y(0, 0)$

$$(\phi_{10} = 0.3, \phi_{01} = 0.3, \sigma^2 = 1.0)$$

	$d_1 = -0.4$ $d_2 = -0.4$	$d_1 = -0.4$ $d_2 = -0.3$	$d_1 = -0.4$ $d_2 = 0.4$	$d_1 = 0.1$ $d_2 = 0.1$	$d_1 = 0.3$ $d_2 = 0.4$	$d_1 = 0.4$ $d_2 = 0.4$
Theoretical Variance $\gamma_Y(0, 0)$	1.1186	1.0914	3.7187	1.4682	6.7996	12.3628
Mean $\bar{\hat{\gamma}}_Y(0, 0)$	1.1118	1.0841	2.5909	1.4404	3.9924	5.2266
Estimated Bias	−0.0068	−0.0073	−1.1278	−0.0278	−2.8072	−7.1362
Absolute Estimated Bias	0.0068	0.0073	1.1278	0.0278	2.8072	7.1362
Estimated Standard Errors	0.0618	0.0607	0.4045	0.0968	0.6103	0.9211
Estimated RMSE	0.0618	0.0608	1.1975	0.1002	2.8721	7.1948

4. The Correlation Function of the FISSAR (1, 1) Process

The autocovariance of the process FISSAR (1, 1) process $\gamma_Y(h_1, h_2)$ is given by (see Shitan [14]),

$$\gamma_Y(h_1, h_2) = \sum_{k=0}^{\infty}\sum_{l=0}^{\infty}\sum_{m=0}^{\infty}\sum_{n=0}^{\infty}\phi_{10}^{k+m}\phi_{01}^{l+n}\gamma_W(h_1 + k - m, h_2 + l - n),$$

where $\gamma_W(\cdot, \cdot)$ is given as,

$$\gamma_W(h_1, h_2) = \sigma^2 \frac{(-1)^{h_1+h_2}\Gamma(1 - 2d_1)\Gamma(1 - 2d_2)}{\Gamma(h_1 - d_1 + 1)\Gamma(1 - h_1 - d_1)\Gamma(h_2 - d_2 + 1)\Gamma(1 - h_2 - d_2)}.$$

The correlation function is given by,

$$\rho(h_1, h_2) = \frac{\gamma_Y(h_1, h_2)}{\gamma_Y(0, 0)}. \tag{7}$$

In Figure 2, the correlation plot for the FISSAR (1, 1) process is shown.

When $d_1 = 0$, and $d_2 = 0$, the FISSAR (1, 1) model reduces to the Standard Separable Autoregressive (SSAR) model, whose correlation function is given as $\phi_{10}^{h_1}\phi_{01}^{h_2}$ (see Shitan [14]). In Figure 3, the correlation plot for the SSAR (1, 1) model is shown.

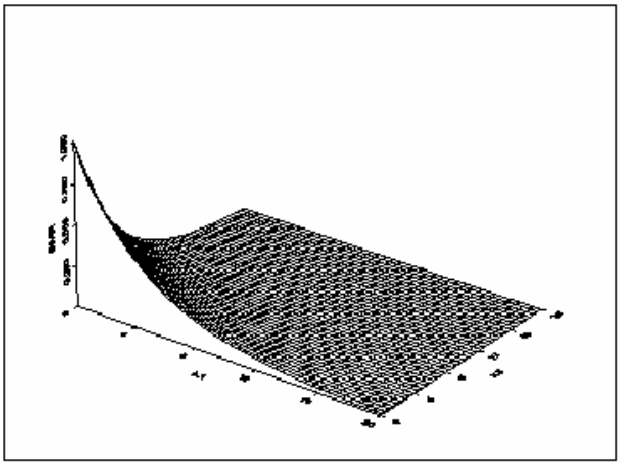

Figure 2. The correlation plot for the FISSAR (1, 1) process.

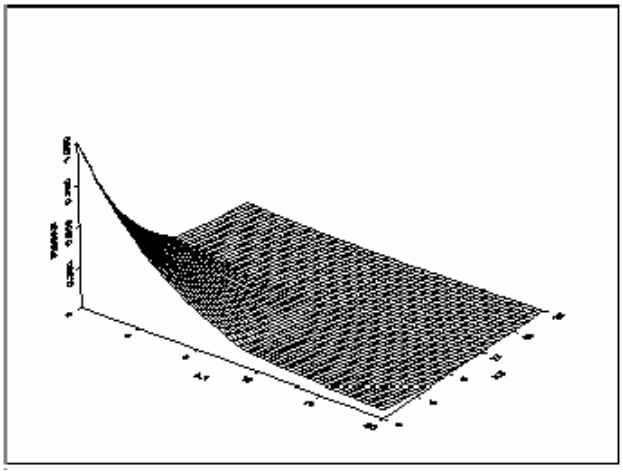

Figure 3. The correlation plot for the SSAR (1, 1) model.

Now, we wish to illustrate graphically that the FISSAR (1, 1) process has a slower decaying correlation structure when compared with SSAR (1, 1) process. One way to do this is to combine the plot of the correlation functions of FISSAR (1, 1) and SSAR (1, 1) into a single graph as shown in Figure 4.

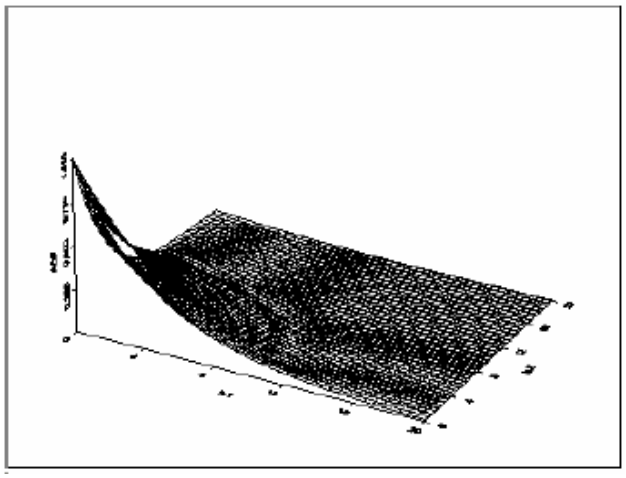

Figure 4. The combined plot of the correlation functions of FISSAR (1, 1) and SSAR (1, 1) process.

However, when these plots are combined into a single graph, it is difficult to distinguish the decaying structure of the two different processes. Hence, in order to clearly see the decaying pattern of the plots, we plotted the correlation functions against h_2, while h_1 was kept fixed at 0, 4, 8, 12, 16, and 20. These plots are shown in Figures 5 to 8. The continuous line refers to the correlation plot of the FISSAR model, while the broken line is the correlation plot of the SSAR process. From these figures, we can clearly see that the FISSAR (1, 1) has a slower decaying property when compared with SSAR (1, 1), thus illustrating its long memory property.

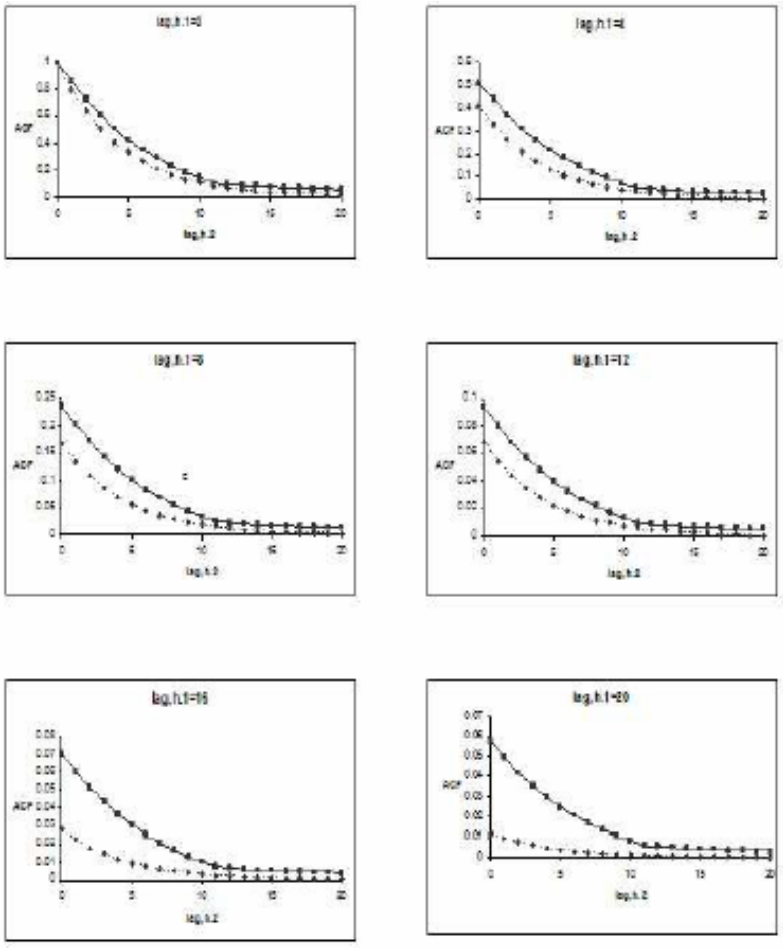

Figure 5. Plot of the correlation functions against h_2, while h_1 was kept fixed at lags 0, 4, 8, 12, 16, and 20 (read across), d_1 = 0.1, d_2 = 0.1, ϕ_{10} = 0.8, ϕ_{01} = 0.8, (FISSAR plot-continuous line, SSAR plot-broken line).

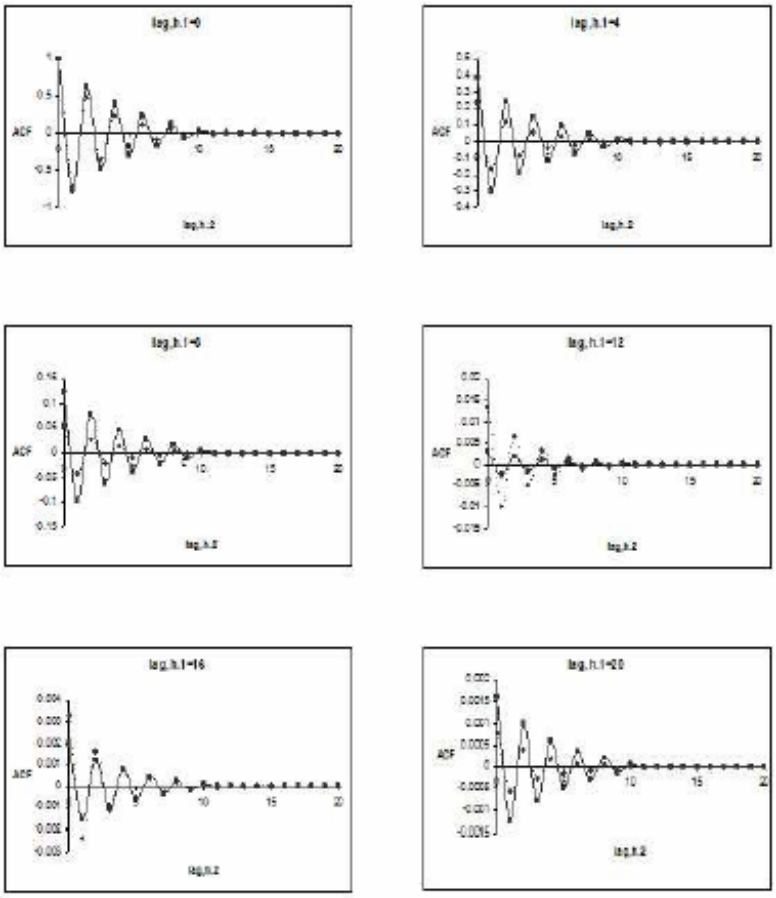

Figure 6. Plot of the correlation functions against h_2, while h_1 was kept fixed at lags 0, 4, 8, 12, 16, and 20 (read across), $d_1 = 0.1$, $d_2 = 0.1$, $\phi_{10} = -0.8$, $\phi_{01} = -0.8$, (FISSAR plot-continuous line, SSAR plot-broken line).

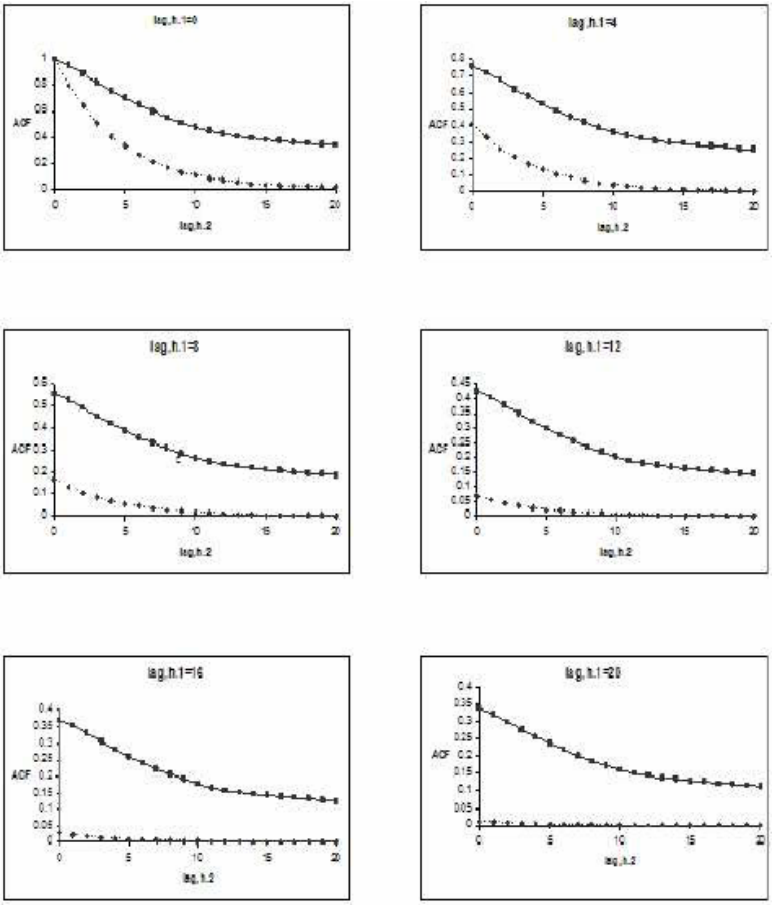

Figure 7. Plot of the correlation functions against h_2, while h_1 was kept fixed at lags 0, 4, 8, 12, 16, and 20 (read across), $d_1 = 0.3$, $d_2 = 0.3$, $\phi_{10} = 0.8$, $\phi_{01} = 0.8$, (FISSAR plot-continuous line, SSAR plot-broken line).

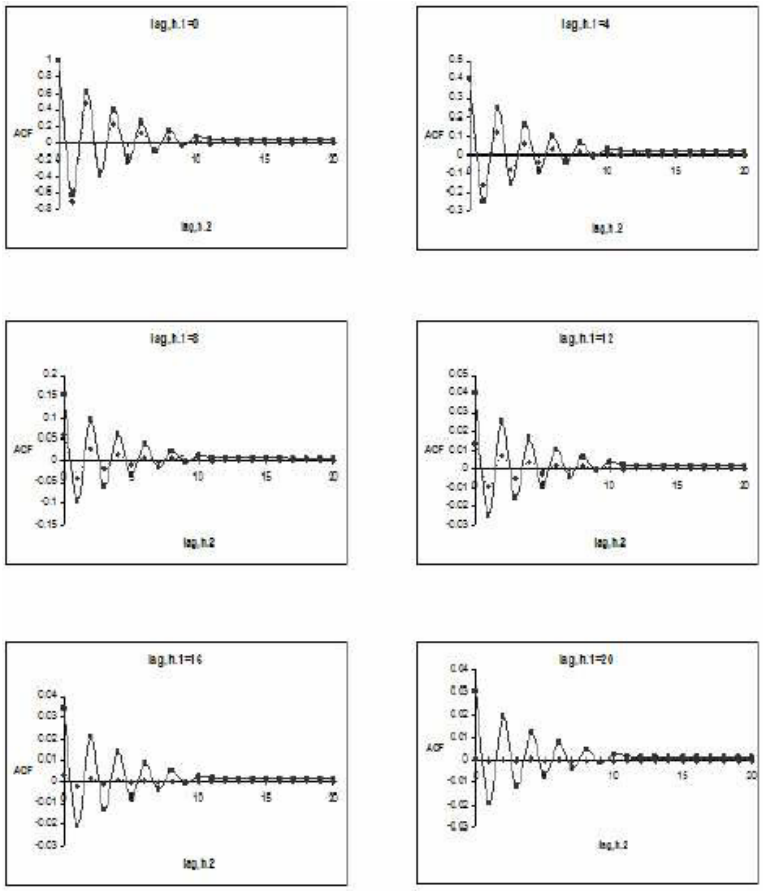

Figure 8. Plot of the correlation functions against h_2, while h_1 was kept fixed at lags 0, 4, 8, 12, 16, and 20 (read across), $d_1 = 0.1$, $d_2 = 0.1$, $\phi_{10} = -0.8$, $\phi_{01} = -0.8$, (FISSAR plot-continuous line, SSAR plot-broken line).

5. Conclusion

The objective of this research was (i) to demonstrate on how to simulate a FISSAR (1, 1) process, (ii) to examine the variance estimator through a simulation study, and (iii) to illustrate graphically the decaying nature of the correlation functions.

Clearly, the sample realisations of FISSAR (1, 1) process can take many different forms and a typical realisation is shown in Figure 1. The ability of the FISSAR process to take on many different forms is useful because it can then be used to model many real life phenomena.

Based on our simulation results, it is found that the numerically computed bias, standard error, and RMSE of the variance estimator provided in Equation (6) were quite small. Hence, this would suggest that this estimator might be a reasonable one.

We have also illustrated graphically that the correlation of the FISSAR process decays at a slower rate than the SSAR process for a given set of parameters. This implies that the FISSAR model would be suitable to model data which have long memory.

References

[1] M. S. Bartlett, Physical nearest neighbour models and non-linear time series, J. Appl. Prob. 8 (1971), 222-232.

[2] I. V. Basawa, P. J. Brockwell and V. M. Mandrekar, Inference for Spatial Time Series, Computer Science and Statistics: Proceedings of the 22nd Symposium on the Interface, Springer-Verlag, New York, (1991).

[3] S. Basu and G. C. Reinsel, Properties of the spatial unilateral first order ARMA models, Adv. Appl. Prob. 25 (1993), 631-648.

[4] J. E. Besag, Spatial interaction and the statistical analysis of lattice systems, J. R. Statist. Soc. B36 (1974), 192-236.

[5] Y. Boissy, B. B. Bhattacharyya, X. Li and G. D. Richardson, Parameter estimates for fractional autoregressive spatial processes, The Annals of Statistics 33(6) (2005), 2553-2567.

[6] P. J. Brockwell and R. A. Davis, Time Series: Theory and Methods, Second Edition, Springer-Verlag, New York, (1991).

[7] P. J. Brockwell and R. A. Davis, Introduction to Time Series and Forecasting, Second Edition, Springer-Verlag, New York, (2002).

[8] C. W. Granger, Long memory relationships and the aggregation of dynamic models, Econometrics 14 (1980), 227-238.

[9] R. P. Haining, The moving average model for spatial interaction, Tran. Inst. Br. Geog. 3 (1978), 202-225.

[10] H. Hurst, Long-term storage capacity of reservoirs, Trans. Amer. Soc. Civil Engrs. 116 (1951), 778-808.

[11] R. J. Martin, A subclass of lattice processes applied to a problem in planar sampling, Biometrika 66 (1979), 209-217.

[12] Mahendran Shitan and Pauline Mah Jin Wee, ARAR and Long Memory Modelling of Tourist Arrivals to Malaysia, Proceedings of National Conference on Management Science and Operations Research, Malacca, 24-25 June (2003), 259-271.

[13] M. Shitan, P. J. W. Mah, Y. S. Lim and Y. C. Lim, Air pollution index determination using ARIMA and ARFIMA time series models, Journal of Engineering Science 2 (2006), 53-60.

[14] M. Shitan, Fractionally integrated separable spatial autoregressive (FISSAR) model and some of its properties, Communications in Statistics Theory and Methods 37 (2008), 1266-1273.

[15] M. Shitan, Corrigendum: Fractionally integrated separable spatial autoregressive (FISSAR) model and some of its properties, Communications in Statistics Theory and Methods 38 (2009), 156-158.

[16] P. Whittle, On stationary processes in the plane, Biometrika 41 (1954), 434-449.

■